Monthly Notices
of the
ROYAL ASTRONOMICAL SOCIETY

Mon. Not. R. Astron. Soc. **403,** 2041–2052 (2010) doi:10.1111/j.1365-2966.2010.16242.x

Optical polarization observations in the Scorpius region: NGC 6124★

M. Marcela Vergne,[1,2,3] Carlos Feinstein,[1,2,3]† Ruben Martínez,[1,3] Ana María Orsatti[1,2,3] and María Paula Alvarez[1]

[1]*Facultad de Ciencias Astronómicas y Geofísicas, Observatorio Astronómico, Paseo del Bosque, 1900 La Plata, Argentina*
[2]*Member of Carrera del Investigador Científico, CONICET, Argentina*
[3]*Instituto de Astrofísica de La Plata, CONICET, Argentina*

Accepted 2009 December 22. Received 2009 December 21; in original form 2009 May 15

ABSTRACT

We have obtained optical multicolour (*UBVRI*) linear polarimetric data for 46 of the brightest stars in the area of the open cluster NGC 6124 in order to investigate the properties of the interstellar medium (ISM) that lies along the line of sight towards the cluster. Our data yield a mean polarization efficiency of $P_V/E(B-V) = 3.1 \pm 0.62$, i.e. a value lower than the polarization produced by the ISM with normal efficiency for an average colour excess of $E(B-V) = 0.80$ as that found for NGC 6124. Besides, the polarization shows an orientation of $\theta \sim 8°.1$ which is not parallel to the Galactic disc, an effect that we think may be caused by the Lupus cloud. Our analysis also indicates that the observed visual extinction in NGC 6124 is caused by the presence of three different absorption sheets located between the Sun and NGC 6124. The values of the internal dispersion of the polarization ($\Delta P_V \sim 1.3$ per cent) and of the colour excess ($\Delta E(B-V) \sim 0.29$ mag) for the members of NGC 6124 seem to be compatible with the presence of an intracluster dust component. Only six stars exhibit some evidence of intrinsic polarization. Our work also shows that polarimetry provides an excellent tool to distinguish between member and non-member stars of a cluster.

Key words: dust, extinction – open clusters and associations: individual: NGC 6124.

1 INTRODUCTION

The open cluster NGC 6124 ($l = 340°.8$, $b = +6°.1$) is an intermediate-richness, detached cluster of slight concentration with stars in a wide range of brightness located in the Scorpius region. This cluster is seen as projected on the edge of a dust cloud which obscures some of its stars, on the north-western part of cluster area. NGC 6124 contains several red giant stars.

This cluster has been studied photoelectrically by Koelbloed (1959), but he only made rough estimates of the distance and of the age of the cluster. In order to get a more accurate determination of those parameters, the study of Koelbloed was extended photoelectrically and photographically to a fainter magnitude limit by Thé (1965). These initial studies of the cluster revealed important discrepancies between the values of the parameters that they obtained. Motivated by some evidence that this cluster is affected by differential reddening, Pedreros (1987) obtained a new set of *UBV* photoelectric observations for NGC 6124 and analysed them using a reddening-line slope adequate for this region of the sky. The distance to NGC 6124 that he estimated using the less evolved stars is 563 ± 10 pc. He also found an age of 1.0×10^8 yr and a mean colour excess of $E(B-V) = 0.80 \pm 0.06$.

A study of the interstellar polarization of NGC 6124 is warranted for three reasons: it provides information on the dust itself; it is a means to trace the Galactic magnetic field and it is also useful to establish cluster membership. The comparison between the polarization and extinction values observed along the same line of sight provides tests for extinction models and grain alignment. The latter involves several processes acting simultaneously, but on different time-scales. The rotating dust grains get a substantial magnetic moment that allows them to precess rapidly about magnetic field lines and, as a result, the grains conserve their orientation relative to that of the magnetic field when the latter fluctuates, forcing the axes of the grains to be aligned with respect to the angular momentum of the grains (Lazarian & Cho 2005). Therefore, the observed polarization vectors map the projected direction of the magnetic field on the plane of the sky, and this allows the investigation of the structure of both the macroscopic field in our Galaxy (Mathewson & Ford 1970; Axon & Ellis 1976) and the local field associated with the individual clouds (Goodman et al. 1990).

Open clusters are very good candidates for polarimetric observations, because many of them have been studied through photometric and spectroscopic techniques and detailed information on the colour, luminosity, spectral type and other properties of their stars is

★Based on observations obtained at Complejo Astronómico El Leoncito (CASLEO), operated under agreement between the CONICET and the National Universities of La Plata, Córdoba, and San Juan, Argentina.
†E-mail: cfeinstein@fcaglp.unlp.edu.ar (CF)

readily available. Thus, the physical parameters of the cluster and its stars can be obtained, and adding polarimetric observations we can study the distribution, size and efficiency of the dust grains which polarize the starlight and the different directions of the Galactic magnetic field along the line of sight to the cluster. As some of the open clusters spread over a significant area, it is possible to analyse the evolution of the physical parameters of the dust over the region. Besides, it is also possible to detect the presence (if any) of intracluster dust and, with additional observations of non-member stars in the same region, to investigate the interstellar dust distribution along the line of sight to the cluster. Finally, the polarimetric data can be used to detect the location of any energetic phenomenon that may have occurred in the history of a cluster (Feinstein et al. 2003), and very important byproducts of these studies are the detection of stars displaying polarization of non-interstellar origin, such as stars with extended atmospheres (e.g. Be stars), and of dust associated to possible binary systems or surrounding the stars (due to evolution or as a formation remnant).

Here, we present multicolour (*UBVRI*) measurements of linear polarization vectors for stars observed in the direction to NGC 6124, and we use them to investigate the properties of the dust located along the line of sight to the cluster . In the following sections, we will discuss the observations, the data calibrations and the results obtained both for the individual stars and for the cluster as a whole.

2 OBSERVATIONS AND DATA REDUCTION

The linear optical polarimetry was obtained during several observing runs at the CASLEO in San Juan, Argentina, during 2003–2007. The Torino five-channel photopolarimeter (Scaltritti et al. 1989; Scaltritti 1994) was used on the 2.15-m telescope. All observations were obtained simultaneously through the five Johnson–Cousins broad-band *UBVRI* filters centred at $\lambda_{\rm Ueff} = 0.360\,\mu$m, $\lambda_{\rm Beff} = 0.440\,\mu$m, $\lambda_{\rm Veff} = 0.530\,\mu$m, $\lambda_{\rm Reff} = 0.690\,\mu$m and $\lambda_{\rm Ieff} = 0.830\,\mu$m. Standard stars for null polarization and for the zero-point of the polarization position angle (PA) were observed several times each night for calibration purposes. The instrumental polarization (IP) was obtained from the null polarization standards and subsequently used to correct the values derived for the programme stars. Polarization standards were used to refer the observed polarization angles to the equatorial system. Table 1 shows the average of the observations of the null polarization standards. Only in the last run, a correction for IP on the *U* filter was needed. For the other filters, the value of the IP was of the same order of magnitude of the observational errors which means that the IP is either negligible or so low that it cannot be determined.

The polarimetric observations are listed in Table 2 which shows, in self explanatory format, the stellar identification as given by Koelbloed (1959), the polarization percentage (P_λ) and the PA of the electric vector (θ_λ) through each filter, as well as their respective mean errors computed considering the photon shot noise as the dominant source of errors (Maronna, Feinstein & Clocchiatti 1992). Since the Torino photopolarimeter collects photons simultaneously in all the filters (*UBVRI*), the final data from each filter may be of different quality, especially those in the *U* band. Therefore, observations whose values were below the 3σ level were ruled out and are not included in Table 2. Three stars (6, 9, and 31) were not rejected, and are included in Table 2 although their measurements showed high errors, because they are evidently low-polarization stars located near the Sun.

A total of 46 stars were polarimetrically observed in the area of NGC 6124. We have 21 stars in common with the photoelectric observations of Pedreros (1987) and other six stars that were quoted as red giants by Koelbloed (1959). The membership information for each star, indicated in the first column of Table 2, was obtained from Pedreros (1987), Thé (1965), Baumgardt, Dettbam & Wielen (2000) and from the WEBDA (http://www.univie.ac.at/webda/). Note, however, that not all the stars observed for the present work have membership information.

3 RESULTS

The sky projection of the *V*-band polarization vectors for the observed stars in NGC 6124 is shown in Fig. 1. The dashed line superimposed to the figure is indicating the orientation of the projection of the Galactic plane (GP), which has a PA of $\theta_{\rm GP} \sim 44^\circ$. Most of the polarization vectors are not aligned with this direction. This is not the usual finding because dust particles in most aged clusters are expected to have enough time to relax and polarize the light in the same orientation as the GP in the region (Axon & Ellis 1976). Normally this is a sign that a perturbation has happened to the dust (Ellis & Axon 1978).

Fig. 2 shows the relation that exists between P_V and θ_V for members (full points), red giants (starred symbols), non-members (open triangles) and stars without any membership data (open circles). We can see a high scatter in angles, probably as a consequence of the presence of intracluster dust or a patchy structure of dust clouds on line of view to the cluster. Also, we observe a spread in polarization values of $\Delta P_V = 1.3$ per cent in the stars historically considered as members of the cluster (excluding stars 3 and 32 with low polarization values, whose memberships will be analysed in the next sections).

Fig. 3 shows the polarization angle distribution. The majority of the stars have their angles in the range of $-10^\circ < \theta_V < 20^\circ$ (grey bars), and the angle distribution of the polarization vectors of the members (dark bars) has a similar behaviour to that of the total sample, with a $\Delta\theta_V > 20^\circ$ (with a full width at half-maximum $\sim 8\overset{\circ}{.}5$). The mean orientation of the polarization vectors in the cluster

Table 1. Results for zero-polarization standards.

Date Number of observations	*U* Q_U(per cent) $\pm\,\epsilon_{Q_U}$ U_U(per cent) $\pm\,\epsilon_{U_U}$	*B* Q_B(per cent) $\pm\,\epsilon_{Q_B}$ U_B(per cent) $\pm\,\epsilon_{U_B}$	*V* Q_V(per cent) $\pm\,\epsilon_{Q_V}$ U_V(per cent) $\pm\,\epsilon_{U_V}$	*R* Q_R(per cent) $\pm\,\epsilon_{Q_R}$ U_R(per cent) $\pm\,\epsilon_{U_R}$	*I* Q_I(per cent) $\pm\,\epsilon_{Q_I}$ U_I(per cent) $\pm\,\epsilon_{U_I}$
2003 April 29–May 2	0.08 ± 0.13	0.10 ± 0.12	0.02 ± 0.06	0.02 ± 0.08	0.03 ± 0.07
12	−0.08 ± 0.2	−0.06 ± 0.13	−0.06 ± 0.131	0.01 ± 0.16	−0.07 ± 0.15
2004 April 18–20	−0.12 ± 0.09	0.06 ± 0.04	−0.02 ± 0.02	−0.001 ± 0.02	−0.011 ± 0.05
5	0.02 ± 0.15	0.03 ± 0.05	0.05± 0.07	0.002± 0.03	0.006± 0.05
2007 May 21–24	−0.24 ± 0.01	−0.01 ± 0.01	−0.09 ± 0.07	−0.03± 0.05	−0.04 ± 0.05
6	−0.190 ± 0.03	−0.08 ± 0.02	0.03 ± 0.06	0.006 ± 0.07	0.012 ± 0.14

Table 2. Polarimetric observations of stars in NGC 6124.

Star Id. Filter	$P_\lambda \pm \epsilon_P$ (per cent)	$\theta_\lambda \pm \epsilon_\theta$ (°)
Star 1 (rg)		
U	2.91 ± 0.69	2.4 ± 6.7
B	4.05 ± 0.31	8.4 ± 2.2
V	3.36 ± 0.23	6.4 ± 2.0
R	3.74 ± 0.21	4.9 ± 1.6
I	3.30 ± 0.28	4.0 ± 2.4
Star 2		
U	2.95 ± 0.15	3.3 ± 1.4
B	3.67 ± 0.14	3.9 ± 1.1
V	3.42 ± 0.26	4.8 ± 2.2
R	3.44 ± 0.17	4.5 ± 1.4
I	3.18 ± 0.20	5.8 ± 1.8
Star 3 (m)		
U	0.77 ± 0.17	13.7 ± 6.2
B	0.92 ± 0.09	15.0 ± 2.7
V	0.89 ± 0.08	15.1 ± 2.5
R	0.98 ± 0.08	13.1 ± 2.2
I	0.90 ± 0.10	13.9 ± 3.1
Star 4		
U	2.54 ± 0.30	15.2 ± 3.4
B	3.46 ± 0.16	11.2 ± 1.3
V	3.35 ± 0.14	8.7 ± 1.2
R	3.56 ± 0.10	9.4 ± 0.8
I	3.13 ± 0.12	8.8 ± 1.1
Star 5 (mP)		
U	2.25 ± 0.22	13.3 ± 2.8
B	2.68 ± 0.17	11.2 ± 1.8
V	2.77 ± 0.15	12.2 ± 1.5
R	2.70 ± 0.12	11.4 ± 1.3
I	2.62 ± 0.15	10.4 ± 1.6
Star 6 (nP)		
U	0.46 ± 0.33	56.6 ± 17.7
B	0.23 ± 0.27	83.4 ± 24.7
V	0.11 ± 0.34	82.6 ± 36.0
R	0.08 ± 0.17	92.1 ± 32.0
I	0.14 ± 0.20	66.2 ± 27.7
Star 7		
U	2.05 ± 0.28	8.5 ± 3.8
B	2.33 ± 0.25	10.4 ± 3.0
V	2.09 ± 0.32	13.0 ± 4.3
R	2.03 ± 0.22	12.7 ± 3.0
I	1.73 ± 0.25	7.8 ± 4.1
Star 8 (mP)		
U	1.67 ± 0.19	13.0 ± 3.3
B	2.09 ± 0.13	8.6 ± 1.7
V	1.95 ± 0.12	9.6 ± 1.7
R	2.02 ± 0.10	9.4 ± 1.5
I	1.75 ± 0.14	8.3 ± 2.3
Star 9 (n)		
U	0.65 ± 0.34	57.9 ± 13.8
B	0.19 ± 0.18	42.5 ± 22.4
V	0.23 ± 0.13	99.6 ± 14.5
R	0.05 ± 0.12	130.4 ± 33.0
I	0.09 ± 0.17	160.1 ± 31.4
Star 10		
U	1.67 ± 0.36	0.1 ± 6.1
B	1.87 ± 0.32	5.3 ± 4.8
V	1.76 ± 0.34	8.2 ± 5.5
R	1.71 ± 0.21	11.3 ± 3.5
I	1.62 ± 0.29	13.5 ± 5.1

Table 2 – *continued*

Star Id. Filter	$P_\lambda \pm \epsilon_P$ (per cent)	$\theta_\lambda \pm \epsilon_\theta$ (°)
Star 11		
U	2.60 ± 0.22	179.6 ± 2.4
B	2.88 ± 0.10	0.6 ± 1.0
V	3.03 ± 0.15	178.9 ± 1.4
R	3.04 ± 0.11	178.8 ± 1.0
I	2.72 ± 0.17	177.9 ± 1.8
Star 12		
U	2.06 ± 0.56	5.9 ± 7.6
B	2.06 ± 0.17	177.3 ± 2.3
V	2.44 ± 0.27	173.6 ± 3.2
R	2.48 ± 0.23	174.6 ± 2.7
I	2.05 ± 0.27	174.6 ± 3.8
Star 13 (nP)		
U	1.53 ± 0.25	4.1 ± 4.6
B	1.84 ± 0.19	1.4 ± 3.0
V	1.76 ± 0.22	170.5 ± 3.6
R	1.90 ± 0.19	172.3 ± 2.9
I	1.65 ± 0.22	168.7 ± 3.7
Star 14 (rg)		
U	3.41 ± 0.87	12.0 ± 7.1
B	2.44 ± 0.29	7.6 ± 3.4
V	2.52 ± 0.26	5.8 ± 3.0
R	2.64 ± 0.22	7.4 ± 2.4
I	2.18 ± 0.28	6.5 ± 3.6
Star 15 (mP)		
U	2.29 ± 0.28	178.6 ± 3.5
B	2.44 ± 0.16	3.0 ± 1.8
V	2.53 ± 0.18	1.6 ± 2.0
R	2.68 ± 0.13	2.2 ± 1.4
I	2.25 ± 0.16	0.3 ± 2.1
Star 16 (mP)		
U	1.31 ± 0.30	176.6 ± 6.5
B	1.58 ± 0.09	177.6 ± 1.6
V	1.54 ± 0.11	176.0 ± 2.1
R	1.60 ± 0.09	175.1 ± 1.6
I	1.41 ± 0.13	173.9 ± 2.6
Star 17		
U	1.94 ± 0.51	6.6 ± 7.3
B	1.75 ± 0.25	1.9 ± 4.0
V	1.59 ± 0.15	5.9 ± 2.7
R	1.56 ± 0.10	2.4 ± 1.9
I	1.33 ± 0.18	2.1 ± 3.9
Star 18 (mP)		
U	1.64 ± 0.19	7.6 ± 3.3
B	1.87 ± 0.15	7.7 ± 2.3
V	1.89 ± 0.18	7.5 ± 2.7
R	1.90 ± 0.15	5.9 ± 2.2
I	1.36 ± 0.20	6.1 ± 4.3
Star 19		
U	1.29 ± 0.31	178.3 ± 6.6
B	2.32 ± 0.10	177.5 ± 1.3
V	2.30 ± 0.12	175.4 ± 1.5
R	2.43 ± 0.09	175.4 ± 1.0
I	2.11 ± 0.11	176.0 ± 1.5
Star 20 (nP)		
U	1.36 ± 0.23	7.1 ± 4.8
B	1.67 ± 0.13	4.2 ± 2.3
V	1.57 ± 0.14	2.7 ± 2.5
R	1.61 ± 0.12	2.6 ± 2.2
I	1.48 ± 0.16	0.3 ± 3.2

Table 2 – *continued*

Star Id. Filter	$P_\lambda \pm \epsilon_P$ (per cent)	$\theta_\lambda \pm \epsilon_\theta$ (°)
Star 21 (mP)		
U	1.94 ± 0.35	5.1 ± 5.1
B	2.33 ± 0.10	5.0 ± 1.3
V	2.27 ± 0.10	3.2 ± 1.2
R	2.40 ± 0.06	4.6 ± 0.8
I	2.24 ± 0.09	5.6 ± 1.2
Star 22 (nP)		
U	2.06 ± 0.47	7.4 ± 6.5
B	2.36 ± 0.16	3.2 ± 1.9
V	2.41 ± 0.15	5.5 ± 1.8
R	2.46 ± 0.13	5.0 ± 1.5
I	2.32 ± 0.15	5.2 ± 1.9
Star 23 (P)		
U	1.53 ± 0.20	4.9 ± 3.8
B	1.65 ± 0.12	7.4 ± 2.1
V	1.82 ± 0.13	5.3 ± 2.1
R	1.76 ± 0.09	3.8 ± 1.5
I	1.60 ± 0.13	1.8 ± 2.4
Star 24 (mP)		
U	1.63 ± 0.21	0.0 ± 3.6
B	1.95 ± 0.16	3.5 ± 2.4
V	2.05 ± 0.12	4.0 ± 1.6
R	2.07 ± 0.13	2.4 ± 1.8
I	1.75 ± 0.18	1.8 ± 3.0
Star 25		
U	1.48 ± 0.16	10.8 ± 3.0
B	1.71 ± 0.07	12.4 ± 1.2
V	1.65 ± 0.08	12.2 ± 1.4
R	1.72 ± 0.06	10.7 ± 0.9
I	1.43 ± 0.10	10.6 ± 2.0
Star 26 (nP)		
U	2.08 ± 0.33	179.8 ± 4.5
B	2.46 ± 0.30	7.0 ± 3.5
V	2.44 ± 0.40	11.9 ± 4.6
R	2.30 ± 0.34	11.1 ± 4.2
I	2.09 ± 0.33	12.1 ± 4.5
Star 27		
U	0.88 ± 0.19	19.8 ± 5.9
B	1.05 ± 0.10	9.7 ± 2.7
V	1.19 ± 0.12	6.3 ± 3.0
R	1.25 ± 0.16	5.6 ± 3.7
I	1.08 ± 0.17	3.4 ± 4.5
Star 28 (nP)		
U	1.91 ± 0.37	3.9 ± 5.4
B	1.88 ± 0.15	3.2 ± 2.3
V	1.84 ± 0.14	0.8 ± 2.3
R	1.85 ± 0.09	1.8 ± 1.4
I	1.68 ± 0.12	4.4 ± 2.1
Star 29 (rgP)		
U	1.55 ± 1.27	34.2 ± 19.6
B	2.07 ± 0.30	2.5 ± 4.1
V	2.22 ± 0.17	2.9 ± 2.2
R	2.24 ± 0.20	2.4 ± 2.5
I	1.89 ± 0.21	1.5 ± 3.2
Star 30 (m)		
U	2.09 ± 0.34	5.3 ± 4.6
B	2.49 ± 0.20	9.5 ± 2.3
V	2.46 ± 0.15	6.4 ± 1.7
R	2.45 ± 0.13	9.1 ± 1.5
I	1.98 ± 0.26	10.7 ± 3.7

Table 2 – *continued*

Star Id. Filter	$P_\lambda \pm \epsilon_P$ (per cent)	$\theta_\lambda \pm \epsilon_\theta$ (°)
Star 31		
U	0.54 ± 0.34	32.2 ± 16.1
B	0.03 ± 0.12	25.3 ± 39.2
V	0.07 ± 0.13	77.6 ± 30.4
R	0.06 ± 0.14	70.1 ± 33.5
I	0.16 ± 0.15	99.3 ± 21.1
Star 32 (mP)		
U	0.94 ± 0.36	16.5 ± 10.6
B	0.97 ± 0.22	13.5 ± 6.2
V	1.02 ± 0.14	6.9 ± 3.9
R	1.04 ± 0.10	11.0 ± 2.6
I	0.69 ± 0.20	2.7 ± 8.2
Star 33 (rg)		
U	2.54 ± 0.65	3.6 ± 7.2
B	2.96 ± 0.18	16.7 ± 1.7
V	2.78 ± 0.11	15.8 ± 1.1
R	2.90 ± 0.09	16.6 ± 0.9
I	2.48 ± 0.09	15.4 ± 1.0
Star 34 (n)		
U	1.64 ± 0.25	22.6 ± 4.4
B	2.66 ± 0.13	14.7 ± 1.4
V	2.46 ± 0.13	17.2 ± 1.5
R	2.65 ± 0.12	16.1 ± 1.3
I	2.24 ± 0.16	15.3 ± 2.1
Star 35 (rg)		
U	1.49 ± 0.49	1.6 ± 9.0
B	2.48 ± 0.11	2.8 ± 1.3
V	2.39 ± 0.11	4.9 ± 1.3
R	2.49 ± 0.08	4.4 ± 0.9
I	2.18 ± 0.10	4.0 ± 1.3
Star 36 (rg)		
U	4.52 ± 1.25	16.0 ± 7.7
B	2.38 ± 0.25	20.7 ± 3.0
V	2.17 ± 0.20	28.2 ± 2.6
R	2.33 ± 0.22	27.9 ± 2.7
I	2.12 ± 0.23	31.7 ± 3.1
Star 37 (mP)		
U	1.84 ± 0.37	13.0 ± 5.6
B	2.27 ± 0.21	11.9 ± 2.6
V	2.40 ± 0.13	10.1 ± 1.6
R	2.39 ± 0.11	8.0 ± 1.3
I	2.25 ± 0.17	6.5 ± 2.2
Star 38 (mP)		
U	1.21 ± 0.21	3.5 ± 4.9
B	1.51 ± 0.12	9.7 ± 2.3
V	1.71 ± 0.09	9.0 ± 1.6
R	1.64 ± 0.08	9.8 ± 1.4
I	1.58 ± 0.14	7.2 ± 2.4
Star 39 (nP)		
U	1.74 ± 0.19	18.6 ± 3.2
B	2.20 ± 0.10	19.7 ± 1.3
V	2.11 ± 0.09	17.2 ± 1.2
R	2.20 ± 0.07	17.2 ± 0.9
I	2.06 ± 0.09	15.2 ± 1.3
Star 40 (mP)		
U	2.66 ± 0.44	15.7 ± 4.6
B	1.91 ± 0.17	11.5 ± 2.6
V	2.07 ± 0.11	11.7 ± 1.5
R	2.10 ± 0.07	11.0 ± 0.9
I	1.84 ± 0.15	11.3 ± 2.4

Table 2 – *continued*

Star Id. Filter	$P_\lambda \pm \epsilon_P$ (per cent)	$\theta_\lambda \pm \epsilon_\theta$ (°)
Star 41 (rg)		
U	2.31 ± 1.15	22.7 ± 13.2
B	1.85 ± 0.27	5.6 ± 4.2
V	1.58 ± 0.23	10.2 ± 4.1
R	1.69 ± 0.26	11.5 ± 4.4
I	1.58 ± 0.28	11.5 ± 5.1
Star 42 (mP)		
U	2.21 ± 0.22	17.2 ± 2.9
B	2.45 ± 0.18	18.7 ± 2.1
V	2.13 ± 0.08	17.6 ± 1.0
R	2.27 ± 0.11	17.2 ± 1.4
I	2.13 ± 0.11	16.4 ± 1.5
Star 43 (m)		
U	2.26 ± 0.21	14.7 ± 2.6
B	2.82 ± 0.18	17.7 ± 1.8
V	2.97 ± 0.12	18.1 ± 1.2
R	3.04 ± 0.11	17.9 ± 1.0
I	2.77 ± 0.16	19.1 ± 1.7
Star 44 (n)		
U	1.32 ± 0.16	14.7 ± 3.5
B	1.80 ± 0.12	12.0 ± 1.8
V	1.71 ± 0.23	15.3 ± 3.8
R	1.82 ± 0.20	15.3 ± 3.1
I	1.63 ± 0.15	17.0 ± 2.7
Star 45 (n)		
U	1.12 ± 0.31	20.0 ± 7.8
B	1.56 ± 0.17	19.7 ± 3.0
V	1.62 ± 0.14	18.6 ± 2.5
R	1.67 ± 0.12	20.2 ± 2.1
I	1.38 ± 0.23	16.0 ± 4.8
Star 46		
U	1.50 ± 0.18	34.0 ± 3.5
B	1.73 ± 0.12	24.4 ± 1.9
V	1.78 ± 0.17	20.0 ± 2.7
R	1.86 ± 0.13	20.7 ± 2.0
I	1.70 ± 0.16	17.0 ± 2.7

m: member (determination from the literature; see text)
n: non-member
rg: red giant
P: observed by Pedreros (1987).

is $\bar{\theta}_V \sim 8.^\circ1$ (vertical dashed line), but the orientation of the GP in the region is $\theta_{GP} \sim 44^\circ$ (vertical solid line). So both directions differ in ∼36°. All the stars that have $\theta_V > 25^\circ$ are already known non-members.

A group of seven red giant stars (1, 14, 29, 33, 35, 36 and 41) is included in our sample, six of them photoelectrically observed by Koelbloed (1959). According to his data, they are K and M giants and members of the cluster. Pedreros (1987) adopted the photometric data from Koelbloed (1959), and their locations in his colour–colour diagram show that these stars would belong to the cluster. These evolved stars have extended atmospheres, therefore they are candidates to have a non-interstellar component in their polarizations. The polarization value, in the visual filter, of each of the red giant stars is similar (see Table 2), excepting stars 1 and 41 that have extreme polarization values ($P_V = 3.75$ and 1.58 per cent, respectively). The low polarization of the star 41 suggests that it could be depolarized due to the presence of an intrinsic component. The polarization angles of the giant stars are lower than 10°, with the exception of stars 33 and 36. The first one is classified as M0III in the literature, and according to Thé (1965) it can probably be a distant giant M star not belonging to the cluster. The second star (36) has several spectral types in the literature (G2III, G8III, K2III), but according to the Washington Visual Double Catalog (Worley & Douglass 1996), it has a companion with magnitude 14.20 mag. The binary nature of this star could explain the variation of the polarization angle with the wavelength.

4 ANALYSIS AND DISCUSSION

4.1 Serkowski's law

To analyse the data, the polarimetric observations in the five filters were fitted in each star of our sample using Serkowski's law of interstellar polarization (Serkowski 1973). That is

$$P_\lambda / P_{\lambda\max} = \mathrm{e}^{-K\ln^2(\lambda_{\max}/\lambda)}. \quad (1)$$

We will assume that if polarization is produced by aligned interstellar dust grains, the observed data (in terms of wavelength, *UBVRI*) will then follow (1) and each star will have a $P_{\lambda_{\max}}$ and $\lambda_{\max}$ value.

To perform the fitting we adopted $K = 1.66\,\lambda_{\max} + 0.01$ (Whittet et al. 1992). For all stars in the sample, we computed the σ_1 parameter (the unit weight error of the fit) in order to quantify the departure of our data from the 'theoretical curve' of Serkowski's law. In our scheme, when a star shows $\sigma_1 > 1.5$, it is indicating the presence of intrinsic stellar polarization. Also, $\lambda_{\max}$ values can be used to test the origin of the polarization: those stars which have $\lambda_{\max}$ much lower than the average value of the interstellar medium (ISM) (0.545 μm; Serkowski, Mathewson & Ford 1975) are candidates to have an intrinsic component of polarization as well. Another criterion to detect intrinsic stellar polarization comes from computing the dispersion of the PA for each star normalized by the average of the PA errors ($\bar{\epsilon}$). The values obtained for $P_{\lambda_{\max}}$, the σ_1 parameter, $\lambda_{\max}$ and $\bar{\epsilon}$, together with the identification of stars, are listed in Table 3. The expression used to calculate the σ_1 parameter is also shown in the footnote. No star in Table 3 has its $\lambda_{\max}$ much lower than the average for the ISM.

Fig. 4 displays P_λ and θ_λ plots for six stars (13, 26, 27, 36, 42 and 46) with probable indications of intrinsic polarization. The presence of a non-interstellar component in the measured polarization of the light from a star causes a mismatch between observations and the Serkowski's curve fit, and/or a rotation in the PA of the polarization vector. This mismatch is clearly shown in the σ_1 value for star 42 ($\sigma_1 = 1.81$), and its variations in P_λ is a plane curve, indicating more than one component in polarization. In the other five stars, the presence of an intrinsic component of polarization is seen through the variation of $\theta_\lambda(\bar{\epsilon}$ parameter). In particular, the P_U of star 36 is out of the Serkowski's fit and, as it was mentioned before, it is a known binary system.

4.2 Stokes plane and memberships

To analyse the characteristics of the ISM in the region of NGC 6124, we plot the normalized individual Stokes parameters in the visual filter of the polarization vector $\boldsymbol{P}_V$, given by $Q_V = \boldsymbol{P}_V \cos(2\theta_V)$ and $U_V = \boldsymbol{P}_V \sin(2\theta_V)$, which represent the vector's equatorial components, for each of the observed stars. In this figure, the stars are plotted according to the literature with their initial membership status. Filled circles are used for members, open triangles

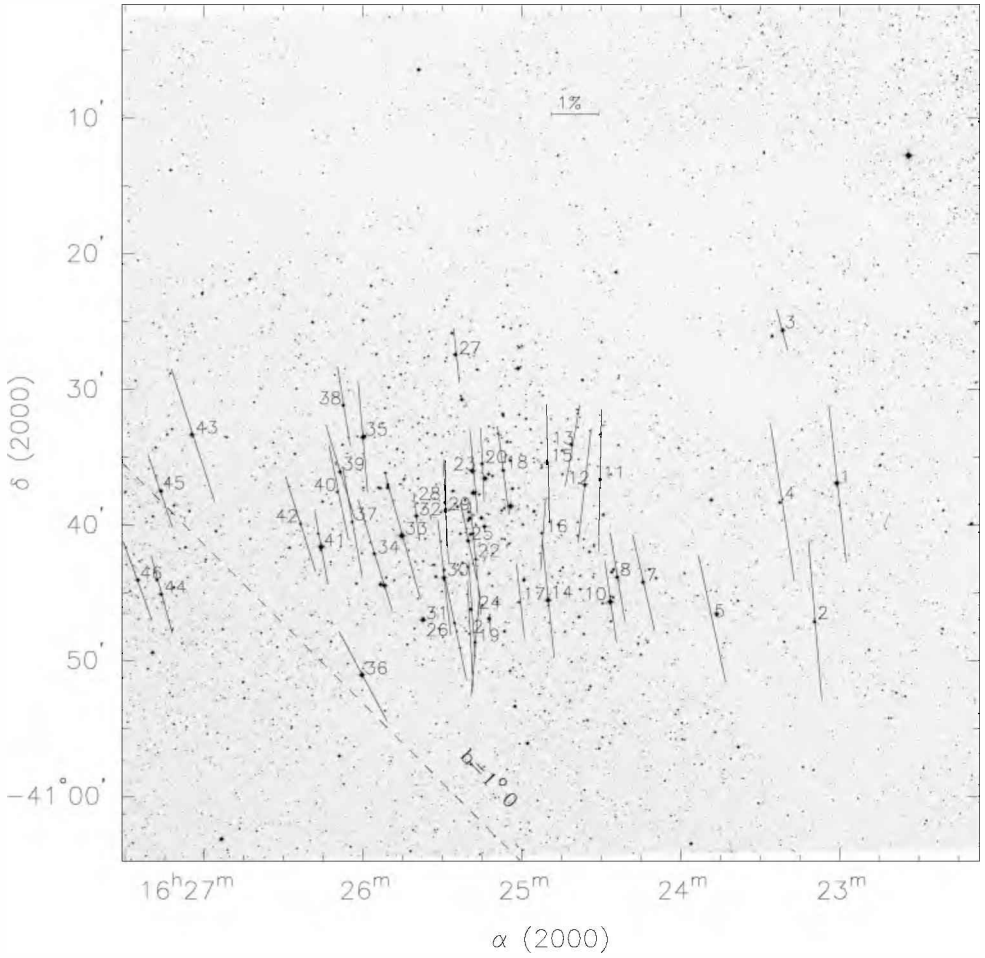

Figure 1. Projection in the sky of the polarization vectors (Johnson V filter) of the stars observed in the region of NGC 6124. The dashed line is the Galactic parallel $b = 1°.0$. This plot shows only the observed stars close to the central core.

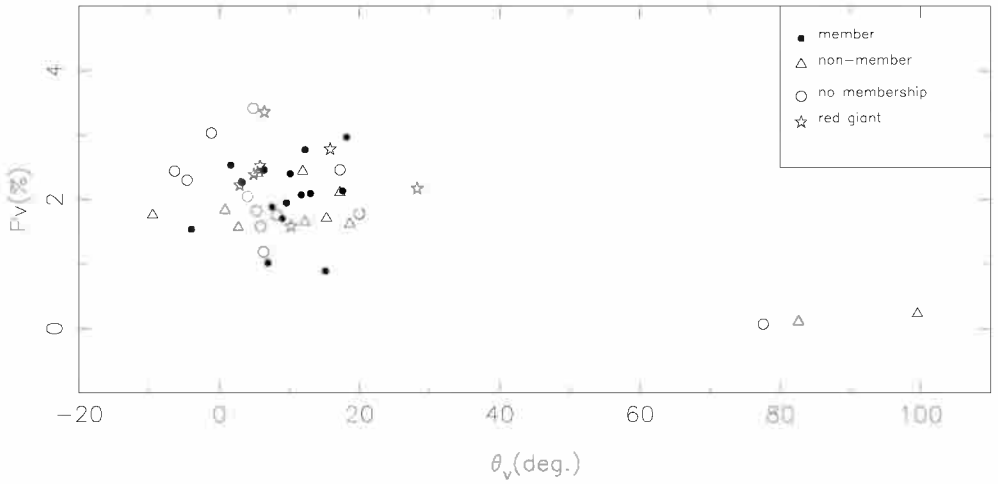

Figure 2. V-band polarization percentage of the stellar flux P_V (per cent) versus the polarization angle θ_V for each star. Symbols indicate the membership classification from the literature. No membership means that there are not previous membership studies.

are used for non-members, starred symbols are used for red giant stars and open circles are used for those stars without membership information.

The polarimetric technique can help to solve membership problems. This type of plot (Q_V versus U_V) used in combination with photometric information is useful to separate members and non-members.

In Fig. 5, the point of coordinates $Q_V = 0$ and $U_V = 0$ indicate the dustless solar neighbourhood, and any other point represents the direction of the polarization vector with modulus $P_V = \sqrt{Q_V^2 + U_V^2}$

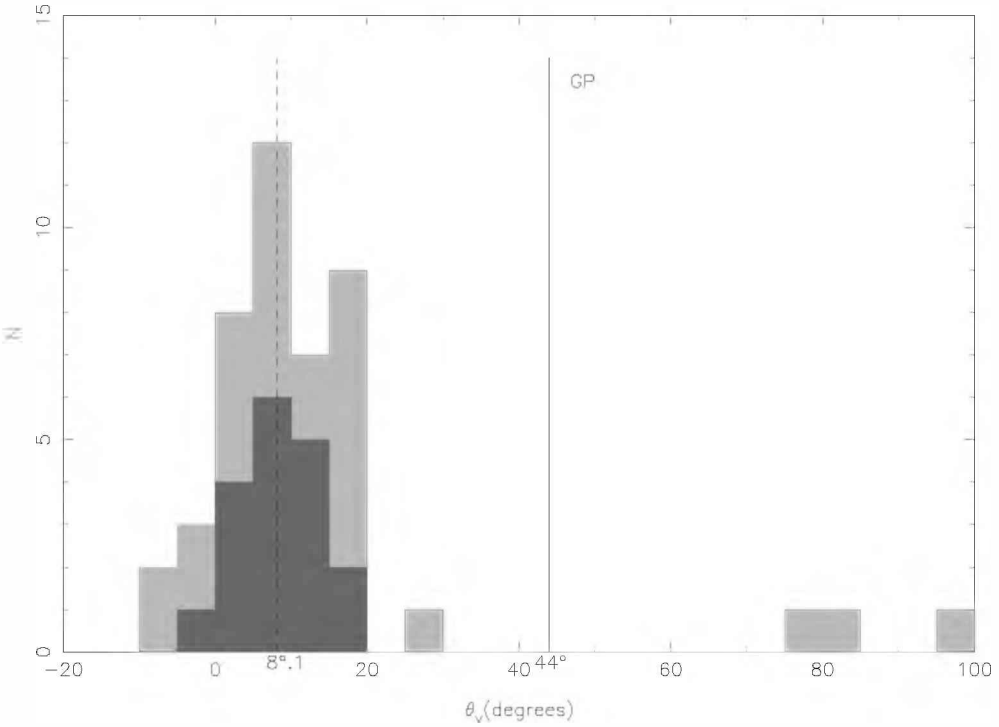

Figure 3. Polarization angle distribution. Grey bars are the histogram for all the stars observed in the region, while the dark ones are for the member stars. The solid line, labelled as GP, is the projection of the GP in the region and the dashed line is the average angle of the polarization vector for the cluster.

as seen from the Sun. Again, this figure shows a high dispersion in angles.

4.2.1 *Stars close to the Sun*

On the left-hand side of the diagram, near point (0,0), there is a group of three stars (6, 9 and 31) with very low polarization values (0.11, 0.23 and 0.07 per cent, respectively). Star 6 was observed by Pedreros (1987) and classified as a non-member of spectral type G5. Star 9, according to Thé (1965), may be a non-member variable star, and star 31 is of spectral type F8V (Houk & Cowley 1975). The low polarization of these stars is compatible with their small reddening. Therefore, they could be confirmed polarimetrically as non-member stars.

Stars 3 and 32 (originally considered as members) have their polarization values of 0.89 and 1.02 per cent, respectively. From its photometric data, star 3 (of spectral type G2V) is located near the Sun (∼100 pc), with an $E(B-V) = 0.08$ mag, compatible with its polarization. In Fig. 1, this star is projected on the north-west side of the sky, where a big dust cloud is observed, obscuring several members on this part of the cluster. Therefore, if it were a member, its light would be expected to be highly polarized, but it is not. For star 32, according to its Q parameter (Schmidt-Kaler 1982), we obtain a F0-4V approximate spectral type and a distance of ∼160 pc. From these data, the polarization of the light of both stars is likely caused in a dust cloud near the Sun, and for that we propose them as non-member stars.

4.2.2 *Non-member stars*

In Fig. 5, there are two groups of non-member stars with different orientations of polarization vectors but with similar values in polarization. There is a group made up of four non-member stars (34, 39, 44 and 45) with mean values $\bar{\theta}_V = 17^\circ$ and $\bar{P}_V = 1.98$ per cent. Koelbloed (1959) suggested that 44 and 45 were members of the cluster with a common spectral type AO, but their reddenings are smaller than those of other A-type stars in the main sequence of the cluster; and besides, 44 is a B8II star according to Houk & Cowley (1975). Also, if we take into account that these four stars are very close in projection in the sky (on the west side; see Fig. 1) and in the Q_V–U_V plane, indicating similar polarimetric characteristics, probably they are polarized by the same dust cloud. From their photometric data, they are situated nearby the cluster (∼400 pc from the Sun) and in front of it. Therefore, we may confirm them polarimetrically as foreground non-member stars. Also, stars 36 (red giant) and 42 (member) could form part of this group, but they show some evidence of a non-interstellar component.

Other two non-member stars, 20 and 28, have very different polarimetric orientations (2.7 and 0.8, respectively) in comparison to the preceding non-members. Both stars are projected on the central part of the cluster (Fig. 1) and to a mean distance of the Sun of approximately 200 pc (from their photometric data). The scatter between the two non-member groups in their PAs ($\Delta\theta_V \sim 16^\circ$) may be showing that the light from these stars is polarized by several overlapped dust components along the line of sight to the cluster, with different orientations of the local magnetic fields.

4.2.3 *Cluster stars*

Most stars in our sample have their Q_V values in the range (1.29, 2.6), with a high scatter in polarization angles. In this range, we observe a group of stars showing some degree of concentration, considered most of them as members in the literature. To derive mean values, in angle and polarization for the cluster, we use seven

Table 3. Parameters of the Serkowski's fit to the linear polarization data for stars in NGC 6124.

Stellar identification	$P_{\max} \pm \epsilon_P$ (per cent)	σ_1^a	$\lambda_{\max} \pm \epsilon_{\lambda_{\max}}$ (mμ)	$\bar{\epsilon}$
1	3.753 ± 0.182	1.392	0.567 ± 0.063	0.85
2	3.636 ± 0.090	1.061	0.559 ± 0.024	0.38
3	0.974 ± 0.024	0.543	0.614 ± 0.033	0.23
4	3.538 ± 0.088	1.266	0.595 ± 0.033	0.93
5	2.826 ± 0.035	0.494	0.592 ± 0.015	0.34
7	2.252 ± 0.047	0.354	0.483 ± 0.016	1.06
8	2.062 ± 0.051	0.849	0.552 ± 0.029	0.55
10	1.867 ± 0.040	0.266	0.526 ± 0.021	3.51
11	3.093 ± 0.020	0.312	0.576 ± 0.008	0.58
12	2.366 ± 0.082	0.641	0.617 ± 0.042	1.49
13	1.894 ± 0.043	0.428	0.576 ± 0.025	9.06
14	2.646 ± 0.127	0.901	0.539 ± 0.054	0.40
15	2.644 ± 0.059	0.745	0.572 ± 0.026	0.62
16	1.633 ± 0.029	0.541	0.562 ± 0.022	0.57
17	1.714 ± 0.075	0.620	0.488 ± 0.036	0.70
18	1.895 ± 0.070	0.781	0.512 ± 0.037	0.22
19	2.400 ± 0.101	1.489	0.605 ± 0.057	0.33
20	1.671 ± 0.040	0.587	0.560 ± 0.029	0.85
21	2.435 ± 0.043	0.943	0.599 ± 0.025	0.30
22	2.518 ± 0.027	0.359	0.599 ± 0.015	0.29
23	1.809 ± 0.017	0.274	0.575 ± 0.011	1.28
24	2.065 ± 0.032	0.430	0.581 ± 0.020	0.53
25	1.749 ± 0.038	0.970	0.546 ± 0.026	0.57
26	2.465 ± 0.031	0.192	0.539 ± 0.012	4.84
27	1.206 ± 0.024	0.283	0.642 ± 0.021	3.85
28	1.942 ± 0.044	0.588	0.546 ± 0.025	0.58
29	2.232 ± 0.048	0.393	0.564 ± 0.028	0.83
30	2.514 ± 0.053	0.558	0.538 ± 0.026	0.81
32	1.050 ± 0.099	0.799	0.516 ± 0.099	1.41
33	2.930 ± 0.084	1.181	0.551 ± 0.031	0.44
34	2.613 ± 0.130	1.715	0.596 ± 0.065	1.12
35	2.535 ± 0.065	1.128	0.559 ± 0.031	0.42
36	2.355 ± 0.094	0.796	0.576 ± 0.054	5.06
37	2.441 ± 0.015	0.185	0.606 ± 0.009	0.90
38	1.688 ± 0.025	0.466	0.623 ± 0.022	0.66
39	2.247 ± 0.046	1.081	0.593 ± 0.028	1.18
40	2.145 ± 0.078	1.310	0.567 ± 0.052	0.23
41	1.754 ± 0.098	0.696	0.553 ± 0.071	1.37
42	2.301 ± 0.096	1.810	0.576 ± 0.057	0.23
43	3.045 ± 0.030	0.402	0.620 ± 0.013	0.49
44	1.829 ± 0.074	0.831	0.602 ± 0.040	1.34
45	1.648 ± 0.048	0.532	0.606 ± 0.041	0.34
46	1.871 ± 0.018	0.254	0.597 ± 0.011	7.96

$^a\sigma_1{}^2 = \sum (r_\lambda/\epsilon_{p_\lambda})^2/(m-2)$, where m is the number of colours and $r_\lambda = P_\lambda - P_{\max} \exp[-K \ln^2(\lambda_{\max}/\lambda)]$

member stars (8, 18, 21, 30, 37, 38 and 40), obtaining $\bar{P}_V = 2.11$ per cent and $\bar{\theta}_V = 8\overset{\circ}{.}2$. The wavelength of maximum polarization for the same group of stars amounts to $\bar{\lambda}_{\max} = 0.57 \pm 0.04\,\mu$m, a value very close to that of the ISM. According to their locations on the Q_V–U_V plane stars 22 and 26 (originally non-members) may be polarimetrically considered now as members.

On the upper side of this group, we find three stars 5, 33 and 43 with polarization values higher than the mean value for the cluster ($P_V = 2.77$, 2.78 and 2.7 per cent, respectively). Star 5, of spectral type B6II/III (Houk & Cowley 1975), is considered as a member by Pedreros (1987), with a 60 per cent of membership probability (Baumgardt et al. 2000). Polarimetrically, it shows characteristics in angle similar to the members of the cluster, in spite of its high polarization value. Its estimated distance, according to the spectral type, is approximately of 570 pc. As mentioned before, star 33 has a spectral type M0III, and probably it is a distant giant not belonging to the cluster. Star 43 (spectral type B2III–IV) is considered a member with a membership probability of 77 per cent (Baumgardt et al. 2000), but the orientation of the polarization vector ($\theta_V = 18\overset{\circ}{.}1$) is very different from the mean value of the cluster. As this star is an evolved object, an intrinsic polarization component may be expected, but our indicators do not show it. Therefore, these three stars may be possible non-members, due to their position in the Q_V–U_V plane.

Stars 11, 12, 13 and 16 are located on the lower side of the Q_V–U_V plane. Star 16 is considered as a member by Pedreros (1987), but its polarization value (1.63 per cent) and orientation ($\theta_V = 176^\circ$) are both lower than the corresponding values of the rest of members. The estimated spectral type for this star, based on photometric data, gives A8V with a $E(B-V) = 0.39$ mag and a distance to the Sun smaller than that of the cluster. In Fig. 1, it lies near stars 20 and 28 on the central part of the cluster and also in the Q_V–U_V plane, which indicates similar polarimetric characteristics in the dust causing the polarization. Polarimetrically, we conclude that star 16 may be a non-member in front of NGC 6124. Stars 11 and 12 have no membership information, and there is a lack of $(U-B)$ values, therefore it cannot make any prediction about it. Polarimetrically, star 11 has a high polarization value to be considered a member, and the orientation of the polarization vector in the star 12 is very different from the $\bar{\theta}_V$ for the cluster. Star 13 displays intrinsic polarization, and its location in the Q_V–U_V plane is clearly of a non-member.

4.2.4 *Background stars*

On the right-hand side of the same figure, three stars (1, 2 and 4) can be seen which are the most polarized in our sample with $P_V =$ 3.36, 3.42 and 3.35 per cent, respectively. On the sky plane (Fig. 1), they are located on the west side of the cluster and to the south of a big dust cloud. Their polarization angles ($\theta_V = 6\overset{\circ}{.}4$, $4\overset{\circ}{.}8$ and $8\overset{\circ}{.}7$, respectively) are similar to the mean value of the cluster. Star 1 was classified as G8III; therefore, it should have $E(B-V) = 0.87$ mag. Originally, it was considered as a member by Pedreros(1987), but its membership probability is lower than 50 per cent (Baumgardt et al. 2000). The other two stars have no membership information. The location of these three stars in the Q_V versus U_V plot shows characteristics of background stars, their light being polarized for a dust component between them and the cluster.

4.3 Polarization efficiency and distribution of interstellar matter

The ratio $P_V/E(B-V)$ is known as the 'polarization efficiency' of the ISM, and it depends mainly on the alignment efficiency, the magnetic field strength and the depolarization due to radiation traversing more than one dust cloud with different field directions.

Fig. 6 displays the relation (P_V versus $E(B-V)$) that exists between the reddening and the polarization produced by the dust grains along the line of sight to NGC 6124. Assuming normal interstellar material characterized by $R = 3.2$, the empirical upper limit relation for the polarization efficiency given by $P_V = RA_V \sim 9E(B-V)$ (Serkowski et al. 1975) is depicted by the solid line in this figure. Indeed, this line represents the maximum efficiency of the polarization produced by the interstellar dust. Likewise, the dotted line $P_V = 3.5E(B-V)^{0.8}$ represents the most recent estimate of the average efficiency made by Fosalba et al. (2002), valid for

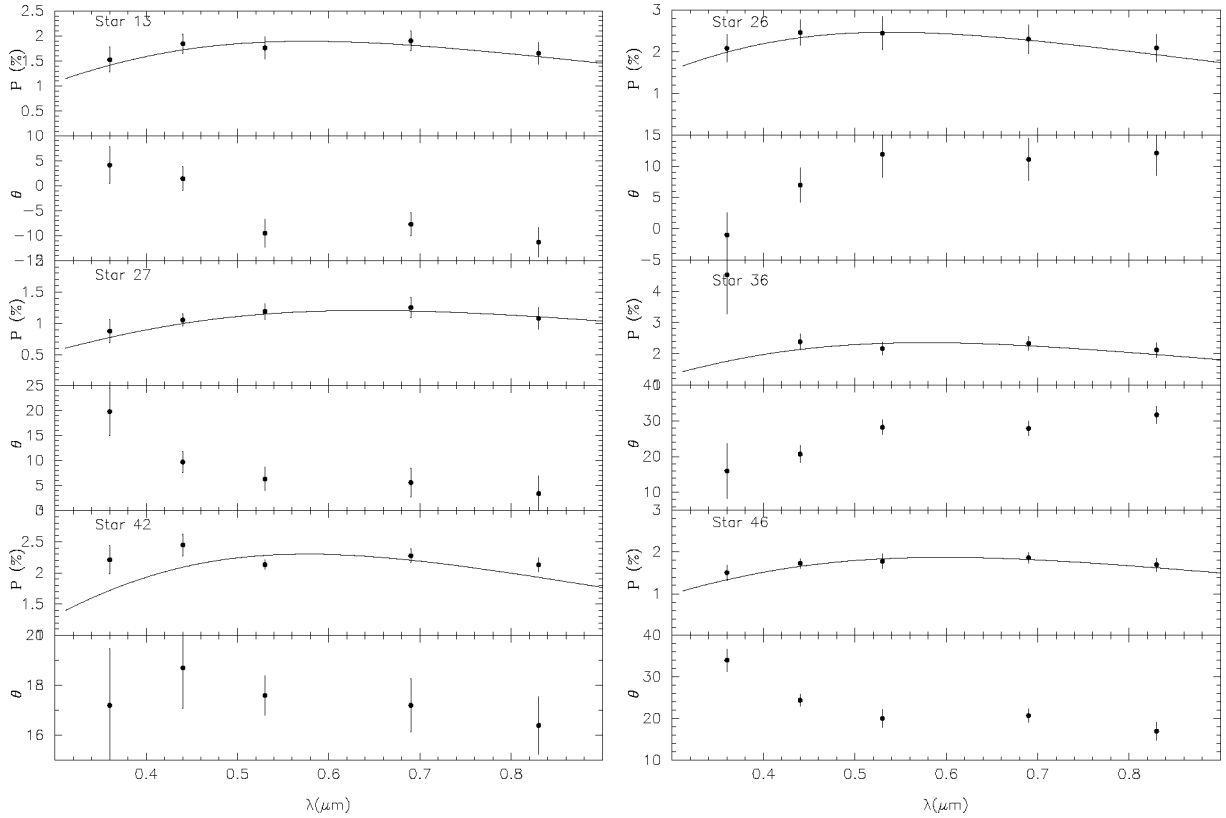

Figure 4. Polarization and PA dependence on wavelength for stars with features of intrinsic polarization.

$E(B-V) < 1.0$ mag. The dashed line $P_V = 5E(B-V)$ was drawn as a reference and represents the observed normal efficiency of the polarizing properties of dust given by Serkowski et al. (1975). In this figure, the stars are plotted with our polarimetric membership status.

Excesses $E(B-V)$ were obtained from the literature or from the relation between spectral type and colour index following Schmidt-Kaler (1982). In Fig. 6, the majority of stars lie on the right of the interstellar maximum efficiency line ($P_V/E(B-V) \sim 9$; Serkowski et al. 1975), indicating that the observed polarization is mostly due to the ISM. Only two stars (3, 28) lie on the left of the line; this can be associated with errors in the estimate of their excesses.

To derive the mean polarimetric efficiency, we made use of the same seven stars that we selected to calculate the mean polarization and angle of NGC 6124 (Section 4.2), located around the cross symbol in Fig. 6. We obtained a mean efficiency $P_V/E(B-V) = 3.1 \pm 0.62$, which is smaller than the value for the interstellar dust given by the Fosalba's estimate ($P_V/E(B-V) \sim 3.66$) and still much smaller than the value given by the Serkowski's estimate ($P_V/E(B-V) \sim 5$) for the average efficiency. This depolarization in the cluster can be the result of the superposition of several dust clouds on the line of sight with different magnetic field directions, confirming the information given in Section 4.1. Also, it shows scattering in colour excess (approximately $0.60 < E(B-V) < 0.89$) and in the polarization values ($\Delta P_V \sim 1.3$ per cent) between members of the cluster. This may be a consequence of the presence of intracluster dust.

Star 32 on the lower side of the figure is probably a late-type star, whose excess may be overestimated. This star is marked in the plot using an arrow that points to smaller excesses. Stars 1 and 33 show low $E(B-V)$ according to the polarization values. Polarimetrically, they are non-member stars with erroneous $E(B-V)$ due to their bad photographic photometry. Again, as mentioned in the preceding section, star 22 shows polarimetric characteristics of a member of the cluster.

In all stars without membership data, it was not possible to calculate their colour excesses. It is the situation for 2, 7, 10, 11, 12, 17, 23, 24, 25, 27, 31 and 46. In the case of stars 7, 12 and 24, they may be considered new probable members of NGC 6124, as their P_V values are similar to those associated with cluster stars. Also, they are located in the region of the Q_V versus U_V plane where there is a number of members. The rest of stars may be probably in the background (like 2 and 11) or nearby non-members (between the Sun and the cluster) like 10, 17, 23, 25, 27, 31 and 46.

4.4 Dust clouds

Our data show that the orientation of the polarimetric vectors is not parallel to the GP (Axon & Ellis 1976) and that there is a considerable degree of depolarization. These two properties can be explained by the composition of the individual effects of several clouds along the line of sight to the cluster, where at least one of these layers of dust polarizes the starlight in an orientation different than the rest, resulting in depolarization. That unusual component might have been recently perturbed so that their dust particles might have not had enough time to relax and to orient in the direction of the GP. The most likely candidate to explain this polarimetric component (and its properties) is the Lupus cloud.

NGC 6124 lies behind the Lupus cloud which is a large structure composed of several subclouds showing different modes

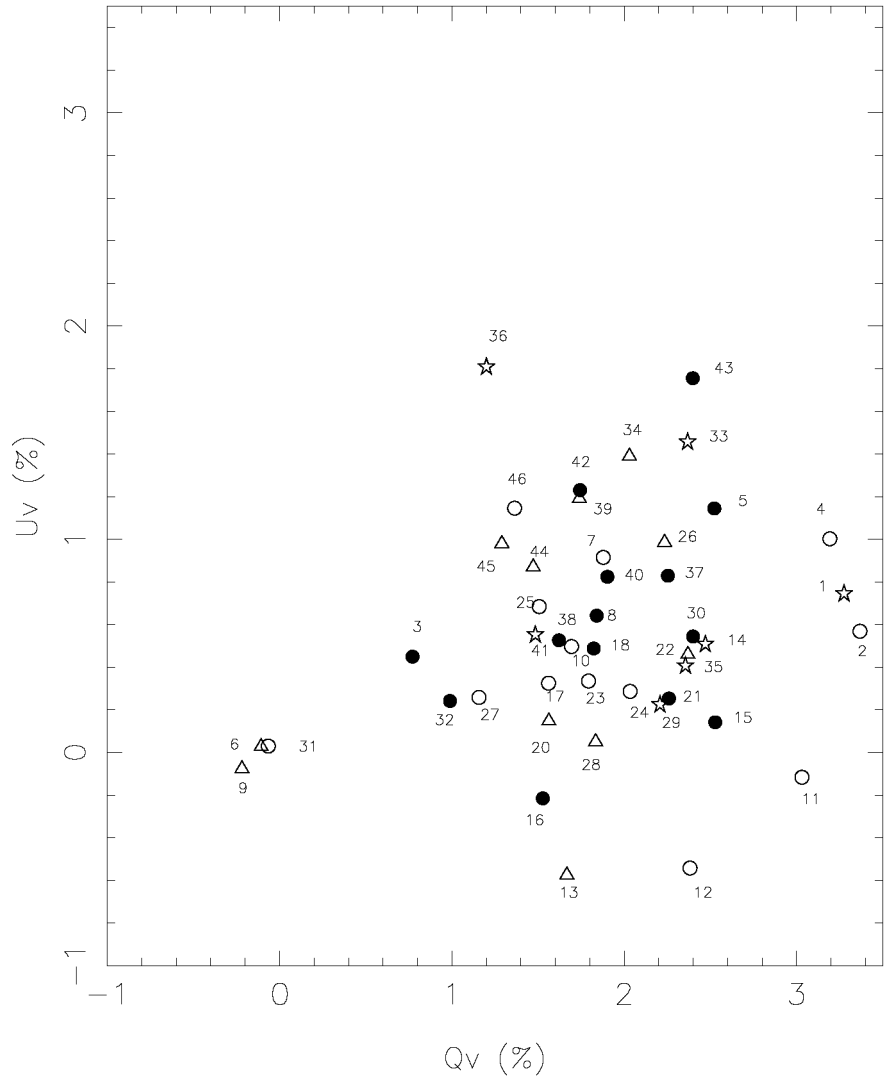

Figure 5. U_V versus Q_V plot for the stars in the region of NGC 6124. Symbols are as in Fig. 2.

of star formation. Applying a maximum-likelihood technique to *Hipparcos* data, Lombardi, Lada & Alves (2008) obtained a distance of $d = 155 \pm 8$ pc, confirming the historical estimate of $d \sim 150$ pc. The subcloud known as Lupus 6 is close to the direction of NGC 6124. The cluster is behind a long dark filament that crosses Lupus 6 and continues up to Lupus 4. Feinstein et al. (2003) have shown that, over the region of NGC 6231, the Lupus cloud does not polarize the light parallel to the GP. The Lupus cloud also stands out as a strong and compact perturbation of the optical polarization of the Galaxy in figs 1(b and c) of Axon & Ellis (1976).

Three non-member stars in the region which seem to be polarized by the Lupus cloud, (16, 20 and 28) give the mean values $\bar{P}_V \sim 1.6$ per cent and $\bar{\theta}_V \sim 0°$. The combination of this orientation and that of the GP ($\theta_V \sim 44°$), close to 90° in the Q_V–U_V plot, could explain the high depolarization of the data. Besides, it could explain the spread of the observations along the Q_V axis (where $\theta_V \sim 0°$), for all lowly polarized stars. As expected, the polarization caused by the Lupus cloud on NGC 6124 is not exactly the same as that for NGC 6231, because the cloud changes its optical properties between the two clusters. In the case of NGC 6231, the observed polarizations for stars 102 and 189 (suspected to be polarized by Lupus) are $P_V = 0.85$ per cent $\pm$ 0.10, $\theta_V = 8\overset{\circ}{.}0 \pm 3.3$ and $P_V = 0.46$ per cent $\pm$ 0.11, $\theta_V = 18\overset{\circ}{.}4 \pm 6.9$, respectively, i.e. somewhat similar in angle, but lower in polarization percentage, to the mean results for the three non-member stars in the NGC 6124 region.

Fig. 7 shows the trend of absorption ($\bar{A}_V$) with increasing distance in the area of NGC 6124. Only stars whose distances were obtained by us are included, and the dot–dashed line accounts for the presence of three absorption sheets between the Sun and NGC 6124 ($d \sim 560$ pc). The first dust component is located very near the Sun and affects stars 3 and 32, but does not produce much extinction ($A_V = 0.2$). Farther out, the absorption increases at about 160 pc (second absorption sheet) as it could be expected from the presence of the Lupus cloud where stars 20 and 28 are located ($A_V \sim 0.5$ mag.). Between approximately 200 and 400 pc there are no stars with known distances but from 400 pc up to the cluster location Fig. 7 shows that the extinction increases considerably, perhaps due to the presence of several dust clouds along the line of sight to the cluster, as mentioned in the preceding sections. A step in the absorption value within the cluster itself can be also noticed and it is probably caused by the presence of an intracluster dust component.

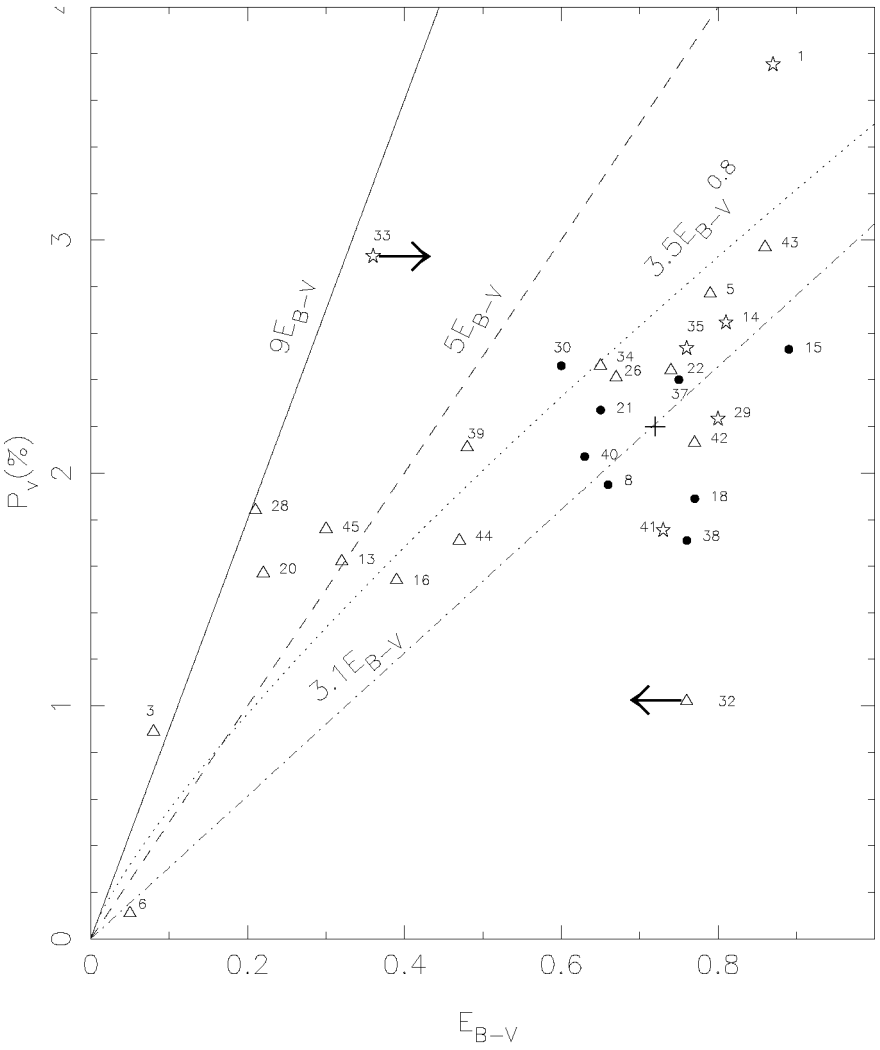

Figure 6. Plot P_V versus E_{B-V} for stars in the region of NGC 6124. From left to right the solid line is the maximum polarimetric efficiency $P_V = 9E_{B-V}$, the dashed line is the Serkowki's estimate average for the Galaxy $P_V = 5E_{B-V}$, the dotted line is the Fosalba's estimate $P_V = 3.5E(B-V)^{0.8}$ and the dot–dashed line is the efficiency found for the cluster $P_V = 3.1E_{B-V}$. Symbols are as in Fig. 2, but the memberships were modified as discussed in Section 4.2.

5 SUMMARY

We obtained the linear polarization of a sample of 46 stars in the region of the open cluster NGC 6124. Through the analysis of our polarimetric data, we have found evidence for at least three dust layers along the line of sight to the cluster.

The average polarization has an angle of $\bar{\theta}_V = 8.^{\circ}2$ which is not parallel to the GP, and the mean polarization efficiency is $P_V/E(B-V) = 3.1$. This value is lower than the average polarization efficiency for the ISM, which means that the cluster is highly depolarized. The scatter in polarization ($\Delta P_V \sim 1.3$ per cent) and in extinction ($\Delta E(B-V) \sim 0.29$ mag) for the members of the cluster is compatible with the presence of intracluster dust.

Our data show that one of these components is associated with the Lupus cloud and that it polarized the light close to $\theta_V = 0^{\circ}$. This orientation differs from the GP projection in the region ($\theta_{GP} = 44^{\circ}$). We interpret that these two different directions of polarizations tend to depolarize the light from the cluster stars because in the Q_V–U_V plane it is basically $2\theta \sim 90^{\circ}$.

We have shown that polarization measurements are useful to detect the non-member stars that contaminate the sample in the NGC 6124 region, and we have been able to detect a few stars with intrinsic polarization.

ACKNOWLEDGMENTS

We wish to acknowledge the technical support at CASLEO during the observing runs. We also acknowledge the use of the Torino Photopolarimeter built at Osservatorio Astronomico di Torino (Italy) and operated under agreement between CASLEO and Osservatorio Astronomico di Torino. We thank Dr Juan Carlos Muzzio for reading of the manuscript and for his useful comments that help to improve this paper. This research has made use of the WEBDA data base, operated at the Institute for Astronomy of the University of Vienna.

REFERENCES

Axon D. J., Ellis R. S., 1976, MNRAS, 177, 499
Baumgardt H., Dettbam C., Wielen R., 2000, A&AS, 146, 251
Ellis R. S., Axon D. J., 1978, Ap&SS, 54, 425

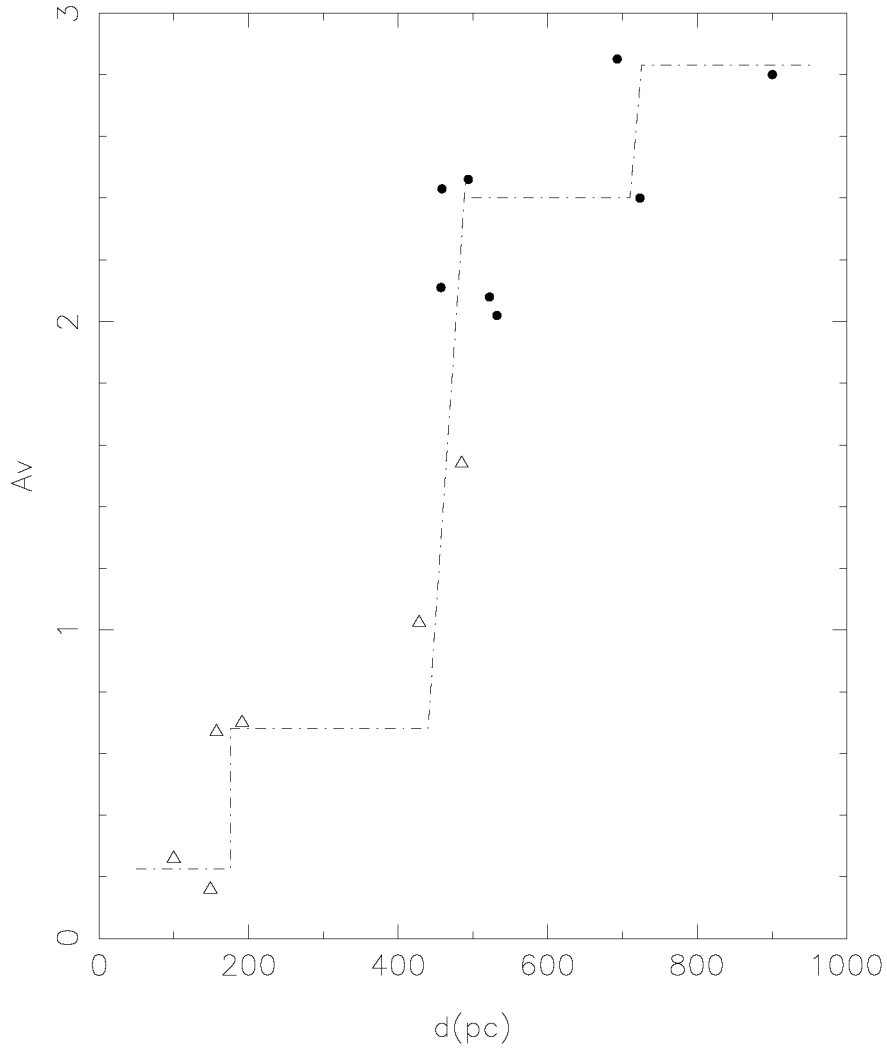

Figure 7. Variation of the absorption (A_V) with increasing distance in the area of NGC 6124. This figure includes only those stars whose distances could be estimated. Open triangles are non-members and solid circles are members.

Feinstein C., Martínez R., Vergne M. M., Baume G., Vázquez R., 2003, ApJ, 598, 349
Fosalba P., Lazarian A., Prunet A., Tauber J., 2002, ApJ, 564, 762
Goodman A. A., Bastien P., Myers P. C., Menard F., 1990, ApJ, 359, 363
Houk N., Cowley A. P., 1975, University of Michigan Catalogue of Two-Dimensional Spectral Types for the HD Stars, Vol. 1. Univ. Michigan, Ann Arbor
Koelbloed D., 1959, Bull. Astron. Inst. Netherlands, 14, 265
Lazarian A., Cho J., 2005, in Adamson A., Aspin C., Davis C. J., Fujiyoshi T., eds, ASP Conf. Ser. Vol. 343, Astronomical Polarimetry: Current Status and Future Directions. Astron. Soc. Pac., San Francisco, p. 333
Lombardi M., Lada C. J., Alves J., 2008, A&A, 480, 785
Maronna R., Feinstein C., Clocchiatti A., 1992, A&A, 260, 525
Mathewson D. S., Ford V. L., 1970, Mem. R. Astron. Soc., 74, 139
Pedreros M., 1987, AJ, 94, 1237
Scaltritti F., 1994, Technical Publication No. TP-001, Osservatorio Astronomica di Torino
Scaltritti F., Piirola V., Cellino A., Anderlucci E., Corcione L., Massone G., Racciopi F., Porcu F., 1989, Mem. Soc. Astron. Ital., 60, 1
Schmidt-Kaler T., 1982, in Schaifers K., Voigt H. H., eds, Landolt-Borstein, Numerical Data and Functional Relationships in Science and Technology New Series, Group VI, Vol. 2, Springer-Verlag, Berlin
Serkowski K., 1973, in Greenberg J. M., van de Hults H. C., eds, Proc. IAU Symp. 52, Interstellar Dust and Related Topics. Reidel, Dordrecht, p. 145
Serkowski K., Mathewson D. L., Ford V. L., 1975, ApJ, 196, 261
Thé P. S., 1965, Contrib. Bosscha Obs. Lembang, 33, 1
Whittet D. C. B., Martin P. G., Hough J. H., Rouse M. F., Nailey J. A., Axon D. J., 1992, ApJ, 386, 562
Worley C. E., Douglass G. G., 1996, A&AS, 125, 523

This paper has been typeset from a TEX/LATEX file prepared by the author.